Chin. J. Astron. Astrophys. Vol. 6 (2006), No. 3, 323–330
(*http://www.chjaa.org*)

Chinese Journal of
Astronomy and
Astrophysics

A One-Dimensional Relativistic Shock Model for the Light Curve of Gamma-ray Bursts *

Cheng-Yue Su[1,2,3], Yi-Ping Qin[1], Jun-Hui Fan[4] and Zhang-Yu Han[5]

[1] National Astronomical Observatories/Yunnan Observatory, Chinese Academy of Sciences, Kunming 650011; *su_cy@163.com*
[2] Graduate School of Chinese Academy of Sciences, Beijing 100049
[3] Department of Physics, Guangdong University of Technology, Guangzhou 530004
[4] Center for Astrophysics, Guangzhou University, Guangzhou 510400
[5] Department of Mechanics, University of Science and Technology of China, Hefei 230026

Received 2005 September 12; accepted 2006 January 10

Abstract We investigate the forming of gamma-ray burst pulses with a simple one-dimensional relativistic shock model. The mechanism is that a "central engine" drives forward the nearby plasma inside the fireball to generate a series of pressure waves. We give a relativistic geometric recurrence formula that connects the time when the pressure waves are produced and the time when the corresponding shocks occurred. This relation enables us to relate the pulse magnitude with the observation time. Our analysis shows that the evolution of the pressure waves leads to a fast rise and an exponential decay pulses. In determining the width of the pulses, the acceleration time is more important than that of the deceleration.

Key words: gamma-ray: bursts — profiles — hydrodynamics — shock waves — methods: numerical

1 INTRODUCTION

Since Gamma-Ray Bursts (GRBs) were first reported in the early 1970's, many important phenomena have been observed (Klebesadel et al. 1973; Norris et al. 1996; Cheng & Lu 2001; also see Zhang & Mészáros 2004; Piran 2004, and references therein). GRBs have a very complex temporal structure with multiple pulses, each comprising a fast rise and an exponential decay (FRED) (Desai 1981; Fishman et al. 1994). Observations revealed that GRBs lie at cosmological distances as their host galaxies show significant redshifts (Cheng & Lu 2001; Zhang & Mészáros 2004). Recently, quite a few authors simultaneously found that GRB 050904 has a very high redshift, up to $z = 6.39^{+0.11}_{-0.12}$ (Haislip et al. 2005; Price et al. 2005; Tagliaferri et al. 2005). GRBs would emit most of energy in the gamma-ray region. The total burst energies are typically in the range of 10^{52}–10^{53} erg at cosmological distances. Isotropic energy up to about 10^{54} erg was detected from GRB 990123. If gamma-ray radiation has a low efficiency, this may suggest that GRBs' emission is beamed as they release so high energies (Mao & Yi 1994). In addition, the polarization and afterglow observed in GRBs also suggest the existence of beaming effect (Piran 2004; and references therein;

* Supported by the National Natural Science Foundation of China.

Hjorth et al. 1999; Sari et al. 1999; Fan et al. 1997). Therefore, beaming models have been widely used to check the observed characters of GRBs (Kulkarni et al. 1999a, b; Huang et al. 2000a).

The GRB phenomena should be stellar charactered (Cheng & Lu 2001). It may be coalescing neutron star binaries, disrupted neutron stars in neutron star-black hole binaries or the collapse of a massive star (Eichler et al. 1989; Woosley 1993). Many characteristics of GRB light curve have been revealed by different authors, using various methods (Norris et al. 1996; Fenimore et al. 1995; Mitrofanov et al. 1996, 1998; Ramirez-Ruiz & Fenimore 1999, 2000; Liang et al. 2002; Qin et al. 2003; Kocevski et al. 2003). In general, the GRB observations can be explained with the fireball model (Goodman 1986; Cavallo & Rees 1978; Shemi & Piran 1990; Paczynski 1990; Dermer et al. 1999). The external and internal shock models interpret respectively the afterglow and the burst (Rees & Mészáros 1992; Mészáros & Rees 1993). In the internal shock model a "central engine" (Fenimore et al. 1993; Rees & Mészáros 1994; Mészáros & Rees 2000) impulses medium to produce the time-varying outflow that leads to a relativistic shock.

People would wish to know what accounts for the profile. Numerical calculations for the evolution of a relativistic fireball have been studied in different ways. Daigne & Mochkovitch (1998, 2000) discussed the internal shocks taking place in a relativistic wind and assumed an inhomogeneous initial distribution of the Lorentz factor and a constant magnetic field. Goodman (1986) and Paczynski (1986) considered the evolution of a fireball. They showed that initially the radiation-pair plasma in a purely radiative fireball behaves like a fluid, and it expands and accelerates under its own pressure, then coasts and decelerates (Kobayashi et al. 1999). Wang et al. (2000) discussed the spectra and time structure in GRBs in terms of the synchrotron radiation of the relativistic electrons to simulate the light curve of GRBs, in which the time scale of the lost energy is about $1 - 10^{-1}$ s in a magnetic field 10^2 Gauss. Kocevski et al. (2003) presented an analytical function of the time profiles of individual GRB pulses that are longer than 2 seconds, with the analytical profiles being independent of the radiative mechanism. Qin et al. (2004) utilized the Doppler effect of the expanding fireball surface to explain the light curve and other characteristics of GRBs. They pointed out that a "local pulse" would be significantly modified by the Doppler effect of the expanding fireball surface.

In this paper, we attempt to present a method for a quantitative analysis of the evolution of the internal shock. We introduce a simple model of the evolution of compression or expansion waves. The method is based on the internal shock model. This mechanism is used to simulate the GRBs' light curve of a simple single-pulse burst. In Section 2 we describe the model, and in Section 3 we present the calculated results. Some conclusions are presented in the last section.

2 DESCRIPTION OF THE MODEL

In the case of GRBs, a radiation-dominated fireball can be considered as an out-flowing fluid (Goodman 1986; Paczynski 1986; Kobayashi et al. 1999). Hinted by the shock model of GRBs, let us consider a very simple case, a one dimensional relativistic shock model, which might provide useful information to explain some GRB light curves which are seen to be pulses comprising the "FRED". In the process of the formation of the fireball the "central engine" (Fenimore et al. 1993; Mészáros 2002) drives the nearby fluid (plasma) inside the fireball to generate a series of pressure waves which propagate in the form of compression waves (Blandford & McKee 1976). These waves will merge with each other to form a shock in a short time. When driving by the "central engine" ceases, which would be corresponding to the onset of deceleration, the fluid near it would give rise to an expansion wave.

In the acceleration stage, the later compression waves travelling more rapidly would overtake the earlier ones, possibly giving rise to a shock. In the case where the later compression waves keep merging into the shock, the pressure and internal energy gradients behind the shock would become stronger and stronger so that the shock wave would get narrower and its velocity would increase rapidly and possibly become relativistic. In contrast, the expansion waves are produced in the deceleration stage. They can also catch up the shock wave (Shapiro 1953; Han & Yin 1993) and keep merging into it. As a result, the shock wave would be lagged and then its magnitude would decline. A single shock pulse will be formed when the two processes are taken into account (Su & Han 2005).

The Lorentz factor of shocks in GRBs can vary from 10 to 10^4 (Piran 2004). If the Lorentz factor of the outflow fluid is γ_b, then when the shock occurs, its Lorentz factor must be greater than γ_b. We then take γ_b

as the critical value of the Lorentz factor: after that $\gamma \geq \gamma_b$ the gamma-ray burst would produce emission such as the synchrotron radiation of relativistic electrons. Let ξ be the efficiency transforming the shock energy to the emission energy, then when ξ can approximately be taken as a constant, the emission intensity of the GRB associated with the shock would increase and decline following the shock magnitude.

3 CALCULATION AND RESULTS

Here, we calculate the shock process numerically. We divide the phase of the "central engine" driving into a large number of sections, each corresponding to a very small time interval Δt. Within each Δt, the physical quantities are assumed to be constants (i.e., they may vary from point to point, but they would not vary with time within this time interval). Obviously, when Δt is small enough, this assumption would hold and the set of these sections could approximately stand for the real process, and when Δt approaches to zero, the set would be exactly the same as the real process.

Let us consider the following situation: the Lorentz factor γ increases linearly within a definite interval in a series of steps (with each step being one of the sections mentioned above) up to some value, $\gamma_m \sim 10^3 - 10^4$ (Kobayashi et al. 1999; Zhang & Mészáros 2004), then it starts to decrease in a series of steps. This process would not influence the evolution of pressure waves (Blandford & McKee 1976). The whole process contains an accelerating stage and a decelerating stage. This gives rise to either compression or expansion waves, and produces the shock wave with a varying magnitude. For the sake of simplicity, we ignore the reverse (or reflected) waves. In the case of a relativistic shock, the jump conditions in the static fluid frame ahead of the shock are as follows (Blandford & McKee 1976)

$$\frac{e_2}{n_2} = \gamma_2 \frac{e_1 + p_1}{n_1}\,, \tag{1}$$

$$\frac{n_2}{n_1} = \frac{\widehat{\gamma}_2\gamma_2 + 1}{\widehat{\gamma}_2 - 1}\,, \tag{2}$$

$$\Gamma^2 = \frac{(\gamma_2 + 1)[\widehat{\gamma}_2(\gamma_2 - 1) + 1]^2}{\widehat{\gamma}_2(2 - \widehat{\gamma}_2)(\gamma_2 - 1) + 2}, \tag{3}$$

where n, e, and p are the density, the energy density, and the pressure, respectively, and γ and Γ are the Lorentz factors of the fluids behind and within the shock, respectively. Here subscript 2 refers fluid parameters behind the shock, and subscript 1, the unshocked fluid ahead of the shock. Quantity $\widehat{\gamma}$, which is not a Lorentz factor, but serves as an isothermal ratio which follows (Blandford & McKee 1976)

$$\widehat{\gamma} = \frac{p}{e - \rho} + 1, \tag{4}$$

where ρ is the rest frame mass density. The isothermal ratio $\widehat{\gamma}$ generally lies between 4/3 (in extreme relativistic cases) and 5/3 (Blandford & McKee 1976; Dai, Huang & Lu 1999; Huang et al. 2000b). These relations, (1)–(4), are applicable to the relativistic shocks. In order to express the Lorentz factor γ_2 as a function of time for the numerical calculation, let us consider a series of steps (the sections) instead of the continue process. Then the equation in the ith step (corresponding to the ith section which is confined within a small time interval Δt), which describes a quantity produced by the ith pressure wave that is impelled by the driving of the "central engine" at the ith step, can simply be obtained by combining Equations (1)–(2). It yields

$$e_2(i) = \gamma_2(i)(e_1 + p_1)\frac{\widehat{\gamma}_2\gamma_2(i) + 1}{\widehat{\gamma}_2 - 1}, \tag{5}$$

where as e_1 and p_1 are parameters of the unshocked fluid ahead of the shock, which we take to be constants. The internal energy and Lorentz factor of the shock induced by the ith pressure wave are respectively $e_2(i)$ and $\gamma_2(i)$. It should be noted the concepts of the ith step and the ith section are slightly different: the ith step means the time of the driving of the "central engine" which produces the ith pressure wave; the ith section means the time interval between the $(i-1)$th and ith waves.

We assign $t_p(i)$ as the time at which the ith pressure waves are produced, and $t_s(i)$, when the ith shock is formed. Then, $t_p(i) = i\Delta t$. Let Δt_p be the time interval during which the "central engine" continuously

drives the fluid to produce two pressure waves (that is, we assign $\Delta t_p = \Delta t$), and Δt_s be the time interval within which these pressure waves give rise to the magnitude variance of the shock. As Δt_p and Δt_s are different, it is necessary to study the relation between them.

Let $l_s(i)$ and $l_p(i)$ be the distances of the moving shock and the "central engine" driving at step i relative to the position where the driving starts; $u(i)$ be the velocity of the pressure wave behind the shock, and $D_s(i)$ be the speed of the shock. With these definitions, one easily obtains $l_s(i)$ from $l_s(i-1)$ by (Su & Han 2005)

$$l_s(i) = l_s(i-1) + D_s(i-1)(t_s(i) - t_s(i-1)) \tag{6}$$

and $l_s(i)$ from $l_p(i+1)$ by

$$l_s(i) = l_p(i+1) + u(i+1)(t_s(i) - t_p(i+1)), \tag{7}$$

where $i > 1$. Note that the pressure wave velocity $u(i)$ is a relativistic combination of the driving velocity and the local speed of sound, a (both speeds being relativistic):

$$u(i) = \frac{(\beta_2(i) + \beta_a)}{(1 + \beta_2(i)\beta_a)} \times c, \tag{8}$$

$$\beta_2(i) = \sqrt{(1 - 1/\gamma_2(i)^2)}, \tag{9}$$

and

$$D_s(i) = c\sqrt{(1 - 1/\Gamma(i)^2)}, \tag{10}$$

where c is the speed of light, and $\beta_a = a/c$. In ultra relativistic cases, $\beta_a = 1/\sqrt{3}$. As mentioned above, $t_p(i) = i\Delta t$, with Δt being the time interval of a step (or a section). All these parameters are defined in the frame of the static fluid ahead of the shock wave. The relation between the energy density e_2 and the shock forming time t_s in each step can then be calculated with Equations (3)–(10).

In the following calculation, the maximum Lorentz factor, $\gamma_{\max}$, is taken from 10, for the lower limit, to 10^3, for the upper limit (Mészáros 2002; Piran 2004). The interval of time for each step is taken as 1 ms, corresponding to $10^{-2} - 10^{-6}$ ms in observation time (one can simply check that the observation time is the $1/2\Gamma^2$ times of the local time). It is thus reasonable that we adopt this local interval time to study the profile of the light curve. However, when a smaller time interval is taken, we obtain a slightly different result, which does not affect our main conclusions. It was suggested that the coasting time and the deceleration time of GRBs are around ~ 10 and ~ 5 s, respectively (see Zhang & Mészáros 2004). We accordingly take $t_{\rm ac} \sim 10$ and $t_{\rm dec} \sim 5$ s as the typical time scales in the acceleration and deceleration stages respectively when illustrating the expected behaviour of the light curve is expected, but, when fitting the light curves of different bursts, various values of $t_{\rm ac}$ and $t_{\rm dec}$ may be taken.

Combining Equations (6) and (7) we obtain

$$t_s(i) = \frac{[l_s(i-1) - D_s(i-1)t_s(i-1) - l_p(i+1) + u(i+1)t_p(i+1)]}{[u(i+1) - D_s(i-1)]}. \tag{11}$$

In this formula, t_s and t_p are well related and t_p could be expressed as a function of t_s:

$$t_p = t_p(t_s). \tag{12}$$

In our calculation, we also defined a driving mode of the " central engine". We assume that γ_2 is a linear function of time, which is the simplest case one may meet. We take

$$\gamma_2(i) = \gamma_b + (\gamma_{\max} - \gamma_b)[t_p(i)/t_{\rm ac}] \quad \text{(for the acceleration stage)}, \tag{13}$$

and

$$\gamma_2(i) = \gamma_b + \gamma_{\max}[t_{\rm dec} + t_{\rm ac} - t_p(i)]/t_{\rm dec} \quad \text{(for the deceleration stage)}, \tag{14}$$

where γ_b and $\gamma_{\max}$ are the initial (the smallest) and the largest Lorentz factors, respectively. We find that other driving modes (i.e., other monotonic functions of acceleration and deceleration) produce roughly the same profile of the light curve.

To provide an intuitive view of the corresponding functions, we present Figure 1, showing the relations between t_p and t_s, between t_p and e_2, and between t_s and e_2. We observe that the first part of the curve in Figure 1a is almost flat, while the last part is extremely steep. This suggests that the relation between t_s and t_p is not a linear one. Figure 1b shows that the shock peaks at the $10th$ s of the driving time t_p, and that at that time the Lorentz factor reaches its maximum and the last compression wave occurs. Note that the curve in Figure 1b is not the real curve of the shock since t_p is not an observed parameter. The driving time t_p corresponds to the shock occurring time t_s (which is the emission time detected by a local observer) is around the 16th second, and so the peak shock will be observed at the 16th second (see Fig. 1c). From Figure 1 we also find that the magnitude of the shock is not a linear function of t_s or t_p.

The expected light curve of the shock can be expressed as

$$f_\nu(t_s) = C_0 \xi e_2(t_s) g_\nu(\nu), \tag{15}$$

where C_0 is a constant, $g_\nu(\nu)$ is the spectrum of the radiation arising from the shock (which might be produced by synchrotron radiation of electrons).

In the case of synchrotron radiation of electrons in an invariable magnetic field, we assume that the count rate within a definite energy channel is proportional to the energy density of the shock and thus the efficiency ξ would be taken as a constant. As we consider only magnitude-normalized light curves, C_0, ξ and $g_\nu(\nu)$ would be cancelled in the following calculation, therefore, the actual values of these quantities are not important in the following analysis.

Let us consider the light curve of shocks in the view of an observer who is located at the spot where the shock occurs (the so-called local observer). In this situation, possible effects such as the curvature effect (the Doppler effect over the whole fireball surface) and the cosmological distant effect could be omitted. Two cases are considered to simulate the light curve of GRBs with the model, which are shown in Figures 2 and 3. For the shorter time scales which correspond to the short GRBs, we obtain very similar results.

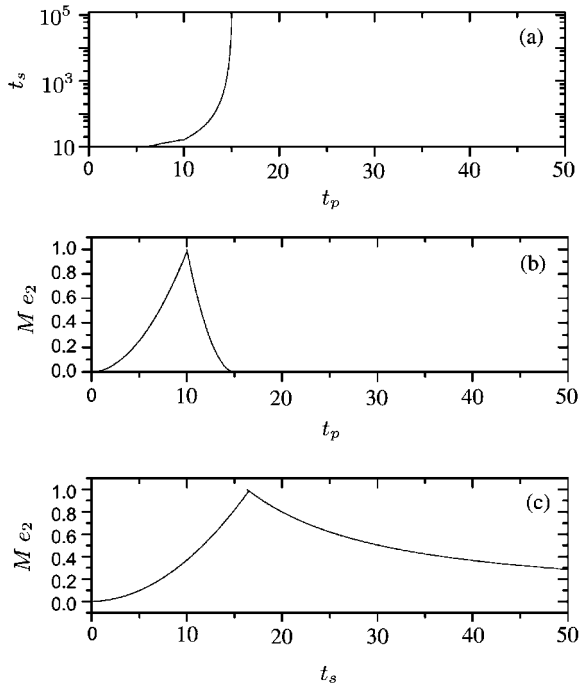

Fig. 1 Relationships between t_p and t_s, (a); t_p and e_2, (b); and t_s and e_2, (c). Here we adopt γ_b=1 and $\gamma_{\max}$=100, and take $t_{\rm ac} = 10$ s and $t_{\rm dec} = 5$ s.

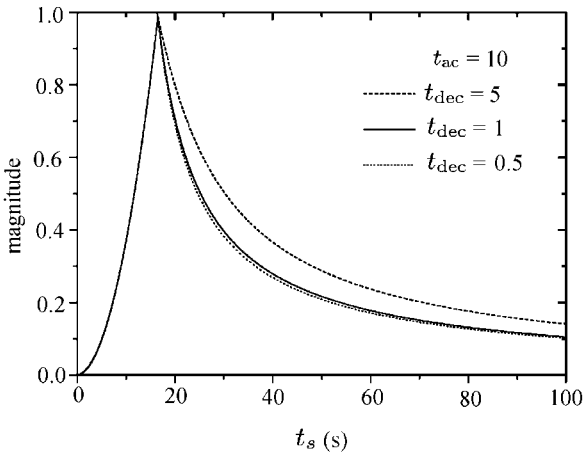

Fig. 2 Simulated GRB light curves for $t_{\rm ac} = 10$ s, and for $t_{\rm dec} = 0.5$ (dotted line), 1 (solid line) and 5 s (dashed line), respectively, and γ_b=1 and $\gamma_{\rm max}$=100.

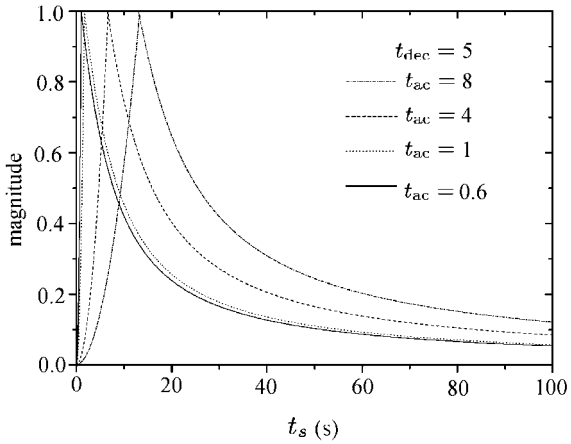

Fig. 3 Simulated GRB light curves for $t_{\rm dec} = 5$ s, and for $t_{\rm ac} = 0.6$ (solid line), 1 (dotted line), 4 (dashed line), and 8 s (dash-dotted line) , respectively, and γ_b=1 and $\gamma_{\rm max}$=100.

4 CONCLUSIONS AND DISCUSSION

In the above sections, we use the evolution of pressure waves to discuss the forming of gamma-ray burst pulses, and find that this mechanism could lead to a "FRED" characteristic of the profile of GRB light curves. As shown in Figure 2, even in the case of $t_{\rm ac} > t_{\rm dec}$, the rising stage of the shock is shorter than the declining stage, which is consistent with the statistical result of GRB light curves discussed previously by some authors (Norris et al. 1996; Liang et al. 2002). We find from Figures 2 and 3 that, in producing the width of pulses, $t_{\rm ac}$ is more important than $t_{\rm dec}$ is. When $t_{\rm ac}$ (or $t_{\rm dec}$) equals to a constant and $t_{\rm dec}$ (or $t_{\rm ac}$) varies from a large value to a small one, it seems that there exists a lower limit for the width of the light curve. Near the peak, the profile looks quite symmetric, but for the entire light curve the profile is not at all symmetric. Hence the temporal symmetry in the short bursts would be interpreted. A significant characteristic of the light curves is that they are quite sharp at the peak. We can conclude that the "FRED" profile could arise from the evolution traits of compression and expression waves. The simulation also fits the light curve of short gamma-ray bursts.

Comparing with the methods of Daigne & Mochkovitch (1998, 2000), we do not introduce the Lorentz factor distribution, but only use the evolution of pressure waves. The success of our method depends on the construction of the relation between $t_p(i)$, the time in which the ith pressure waves are produced, and $t_s(i)$, the time in which the ith shock is formed. This is realized when we employ the relativistic geometric recurrence formula to connect the two quantities (see Equation (11)). Our method is quite natural which does not depend on strict conditions.

Wang et al. (2000) suggested using the synchrotron radiation of relativistic electrons to simulate GRB light curves. In their approach the details of the radiation would be involved. In our model, however, the details of emission are not important in producing the profile of the light curve. Only the shock itself could lead to a "FRED" pulse, regardless the real radiation mechanism. In fact, any radiation involves the efficiency with which the shock energy is transformed into the emission energy, ξ. As long as ξ does not change dramatically, the light curve observed would follow what the shock produces (see Equation (15)). The term $g_\nu(\nu)$ in Equation (15) acts like ξ, which does not significantly alter the light curve observed. The synchrotron radiative efficiency of electrons is generally assumed to be quite small, which is around 1%–5% (Zhang & Mészáros 2004). The efficiency that the energy of shocks transmits to the radiation of electrons was generally taken as 0.2 (see Frail et al. 2001). Note that, the real value of ξ is not important in producing the profile of light curves, as long as it keeps to be invariant.

We observe that, for each source, its variation range of the Lorentz factor and the lasting times of the two stages, acceleration and deceleration, can be adjusted to account for the observations. The critical value associated with a GRB should be unchangeable for the same kind of environment and the same physical mechanism. In our calculation, the evolution of pressure waves is not significantly affected by the actual function of the Lorentz factor as long as it is a monotonic function of time, i.e., the evolution differs only slightly from that associated with a linear function. This agrees with what was mentioned in Blandford & McKee (1976).

Generally, one observes complex profiles rather than simple ones. In the case of the long lasting time bursts, a new shock wave may be produced by the merging of different compression waves behind the shock wave front (Shapiro 1953; Han & Yin 1993), or may be produced by a nonuniform density distribution, or by the repeat action of the "central engine". New shocks will follow the same path of evolution and then form the multiple peaks in the long GRBs.

The sharp characteristic of the light curve profile shown in Figures 2 and 3 is not a common feature observed in GRBs. This is not surprising. Recall that what we discuss above is the light curve of shocks in the view of an observer who is located at the spot where the shock occurs. In the view of a distant observer, what we discussed is merely a local pulse. When taking into account the Doppler effect over the whole fireball surface, a local pulse would be significantly modified. As discussed in detail in Qin et al. (2004), a sharp local pulse would lead to a smooth light curve if its decaying phase is not too short. Our curves belong to this kind of local pulse (see Figs. 2 and 3).

Acknowledgements We thank Professor Wang J. C. for a very helpful discussion and the anonymous referee for invaluable suggestions. This work is funded by the Special Funds For Major State Basic Research Projects, and the National Natural Science Foundation of China (Nos. 10403001, 10125313, 10573005).

References

Blandford R. D., McKee C. F., 1976, Phys Fluids, 19(8), 1130
Cavallo G., Rees M. J., 1978, MNRAS, 183, 359
Cheng K. S., Lu T., 2001, ChJAA, 1, 1
Dai Z. G., Huang Y. F., Lu T., 1999, ApJ, 520, 634
Daigne F., Mochkovitch R., 2000, A&A, 358, 1157
Daigne F., Mochkovitch R., 1998, MNRAS, 296, 275
Dermer C., Bottcher M., Chiang J., 1999, ApJ, 515, L49
Desai U. D., 1981, ApSS, 75, 15
Eichler D., Livio M., Piran T. et al., 1989, Nature, 340, 126
Fan J. H., Cheng K. S., Zhang L., 1997, A&A, 327, 947

Fenimore E. E., Epstein R. I., Ho C. et al., 1993, Nature, 366, 40
Fenimore E. E., in't Zand J. J. M., Norris J. P. et al., 1995, ApJ, 448, L101
Fishman G. J., Meegan C. A., Wilson R. B. et al., 1994, ApJS, 92, 229
Frail D. A., Kulkarni S. R., Sari R. et al., 2001, ApJ, 562, L55
Goodman J., 1986, ApJ, 308, L47
Haislip J., Nysewander M., Reichart D. et al., 2005, astro-ph/0509660
Han Z. Y., Yin X. Z., 1993, Shock Dynamics, Kluwer Academic Publishers Science Press
Huang Y. F., Dai Z. G., Lu T., 2000a, A&A, 355, L43
Huang Y. F., Gou L. J., Dai Z. G. et al., 2000b, ApJ, 543, 90
Hjorth J., Björnsson G., Andersen M. I. et al., 1999, Science, 283, 2073
Klebesadel R., Strong I., Olson R., 1973, ApJ, 182, L85
Kobayashi S., Piran T., Sari R., 1999, ApJ, 513, 669
Kocevski D., Ryde F., Liang E., 2003, ApJ, 596, 389
Kulkarni S. R., Djorgovski S. G., Odewahn S. C. et al., 1999a, Nature, 398, 389
Kulkarni S. R., Frail D. A., Sari R. et al., 1999b, ApJ, 522, L97
Liang E. W., Xie G. Z., Su C. Y., 2002, PASJ, 54, 1
Mao S., Yi I., 1994, ApJ, 424, L131
Mészáros P., 2002, ARA&A, 40, 137
Mészáros P., Rees M. J., 1993, ApJ, 405, 278
Mészáros P., Rees M. J., 2000, ApJ, 530, 292
Mitrofanov I. G., Chernenko A. M., Pozanenko A. S. et al., 1996, ApJ, 459, 570
Mitrofanov I. G., Pozanenko A. S., Briggs W. et al., 1998, ApJ, 504, 925
Norris J., Nemiro R., Bonell J., et al., 1996, ApJ, 459, 393
Paczynski B., 1986, ApJ, 308, L43
Paczynski B., 1990, ApJ, 363, 218
Piran T., 2004, Reviews of Modern Physics, 76, 1143
Price P. A., Cowie L. L., Minezaki T. et al., 2005, astro-ph/0509697
Qin Y. P., Liang E. W., Xie G. Z., et al., 2003, ChJAA, 3, 38
Qin Y. P., Zhang Z. B., Zhang F. W. et al., 2004, ApJ, 617, 439
Ramirez-Ruiz E., Fenimore E. E., 1999, A&AS, 138, 521
Ramirez-Ruiz E., Fenimore E. E., 2000, ApJ, 539, 712
Rees M. J., Mészáros P., 1994, ApJ, 430, L93
Rees M. J., Mészáros P., 1992, MNRAS, 258, 41
Sari R., Piran T., Halpern J. P., 1999, ApJ, 519, L17
Shapiro A. H., 1953, The Dynamics and Thermodynamics of Compressible Flui d Flow, The Ronald Press Company
Shemi A., Piran T., 1990, ApJ, 365, L55
Su C. Y., Han Z. Y., 2005, PNAOC, 2, 1
Tagliaferri G., Antonelli L. A., Chincarini1 G. et al., 2005, astro-ph/0509766
Wang J. C., Cen X. F., Qian T. L. et al., 2000, ApJ, 532, 267
Woosley S. E., 1993, ApJ, 405, 273
Zhang B., Mészáros P., 2004, IJMPA, 19, 2385